M&C 2017 - International Conference on Mathematics & Computational Methods Applied to Nuclear Science & Engineering, Jeju, Korea, April 16-20, 2017, on USB (2017)

Extended Radial Reflector Modeling Capabilities in MPACT

S. Stimpson,[1] B. Collins,[1] A. Godfrey,[1] F. Franceschini,[2] D. Salazar[2]

[1] *Oak Ridge National Laboratory, One Bethel Valley Road, P.O. Box 2008, Oak Ridge, TN 37831-6172*
stimpsonsg@ornl.gov; collinsbs@ornl.gov; godfreyat@ornl.gov

[2] *Westinghouse Electric Co. LLC, 1000 Westinghouse Dr., Cranberry Township, PA 16066*
francef@westinghouse.com; salazada@westinghouse.com

Abstract – *To provide high fidelity multiphysics simulations of nuclear reactors, the Consortium for Advanced Simulation of Light Water Reactors (CASL) is developing the Virtual Environment for Reactor Applications (VERA). MPACT, which is the primary deterministic neutron transport solver, employs the 2D/1D method to solve 3D problems, leveraging 2D method of characteristics (MOC) for radial transport. To this point, full- and quarter-core MPACT cases have used simple radial reflector models consisting of an explicit baffle representation and an assembly-width of moderator along the core periphery. To extend the fidelity of the radial reflector treatment, a new capability has been developed to approximate the modeling of the structural components of the reflector, such as the core shroud, barrel, neutron pads, and vessel. Several different modeling configurations are explored with varying levels of fidelity and computational burden.*

Three 2D problems are analyzed to assess the impact on eigenvalue and pin power distributions throughout a representative cycle starting with fresh fuel: (1) a Watts Bar Unit 1 quarter-core slice, (2) a Krško full-core slice, and (3) an AP1000®† quarter-core slice. The analyses show that the effect on eigenvalue is fairly small, but the effect on pin power is more pronounced, especially locally in the assemblies closest to the periphery, where the maximum pin power difference is nearly 3.5% in the AP1000 case. This impacts subsequent reloads in which some peripheral fuel assemblies are reinserted; this needs to be evaluated in future studies. Future work will also focus on 3D analyses and developing supporting capabilities to estimate vessel fluence.

I. INTRODUCTION

The primary goal of the Consortium for Advanced Simulation of Light Water Reactors (CASL) [1] is to provide high fidelity simulations of nuclear reactor core physics. To accomplish this, CASL is developing the Virtual Environment for Reactor Applications (VERA) [2], which consists of a collection of physics codes and multiphysics coupling drivers. The MPACT code [3,4] is the primary deterministic neutron transport solver in VERA, predominantly employing the 2D/1D method [3,5,6] to solve 3D transport problems. In this approach, the 2D method of characteristics (MOC) is used for each plane to solve the radial transport, and 1D pin-wise nodal methods are used axially [7]. The work presented here focuses on 2D depletion cases, which strictly use coarse mesh finite difference (CMFD)-accelerated MOC.

Several improvements have been made to MPACT and VERA in recent months, some to enhance computational performance, and others to improve accuracy. Until now, the radial reflector models used in VERA included only an explicit baffle representation and a single assembly-width of moderator. While this approach has proven to be successful, there was some question as to how much the other structural components (barrel, neutron pads, vessel, etc.) would impact the solution, particularly with regard to fuel cycle depletion analyses.

This paper presents a simple pin-wise reflector modeling scheme that uses the centroid of each pin to determine if the pin contains structural material. With this scheme, specification of the core barrel, neutron pads, and other structural components is very easy, and the importance of each specification can be quantified. Including components such as the vessel can add a significant amount

* This manuscript has been authored by UT-Battelle, LLC, under Contract No. DE-AC0500OR22725 with the U.S. Department of Energy.

of computational burden as the problem size is notably increased. To prevent this, an approximate model which serves as the default has been implemented to capture most of the effects without increasing the problem size when compared to previous models.

To test this capability, several problems are evaluated. The first is the 2D Watts Bar Unit 1 (WBN1) core model. This includes comparisons to Monte Carlo reference solutions at beginning of life (BOL) and assessments with depletion, comparing the various reflector modeling options. Similar analyses are performed on 2D models of both the Krško and AP1000 reactor models. All cases use the 47-group cross section library developed at Oak Ridge National Laboratory [8]. It is also worth noting that all of these test cases are first cycle cores. Quantifying the effect in subsequent reload cycles is a topic of future analysis.

II. RADIAL REFLECTOR EXTENSIONS

Prior to this work, the radial reflector modeling in MPACT and VERA consisted of the core baffle surrounded by an assembly-width of moderator (baffle-only model). Figure 1 shows the VERA Progression Problem P5-2D quarter core layout [9], which consists of three different enrichment zones showing the baffle and reflector regions on the periphery.

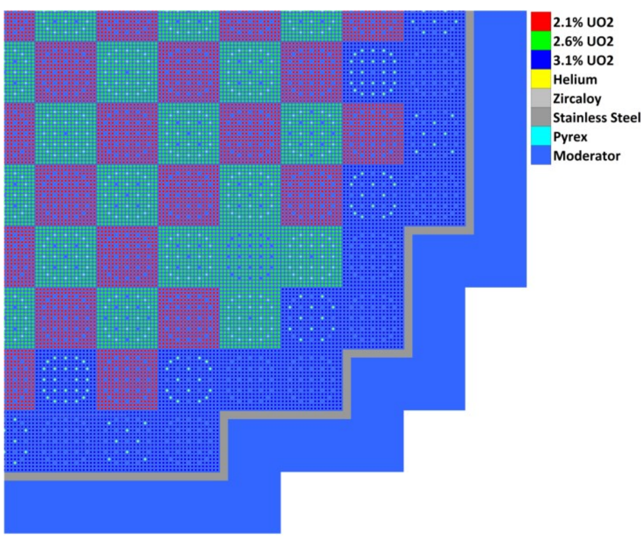

Fig. 1. Geometry visualization of VERA Problem 5a-2D with baffle and moderator reflector region.

In Fig. 1, the reflector regions surrounding the core are still 17 × 17 assemblies, but each pin cell is filled with moderator. To conveniently represent the cylindrical structural components, a routine was implemented to determine if each rod's centroid falls within the inner and outer radii of each cylinder. If so, it is filled with the structural material for that component as specified in the input. For example, Fig. 2 shows the complete radial reflector specification with the core barrel, neutron pad, and vessel. Here the barrel and pad are composed of stainless steel, and the vessel is carbon steel.

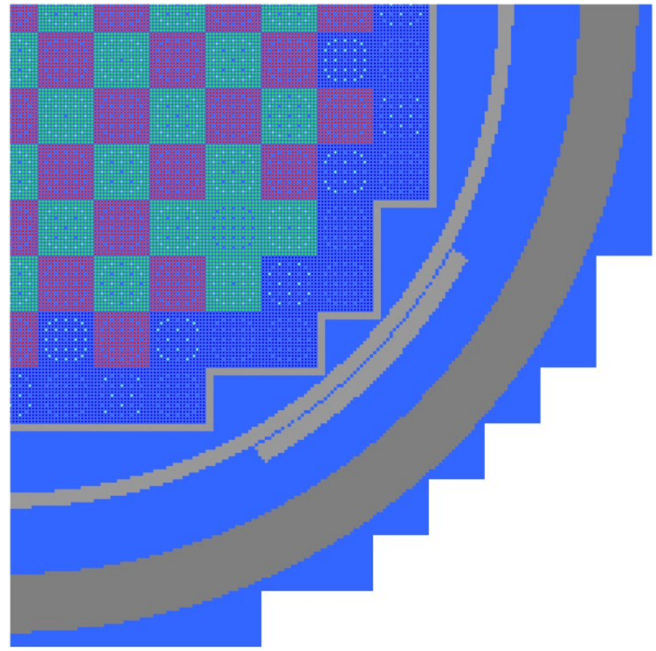

Fig. 2. Geometry visualization of VERA Problem 5a-2D with core barrel, neutron pad, and vessel.

The neutron pad shown in Fig. 2 is not a full cylinder; it is only an arc over a certain range. To specify this, VERA users provide an arc length for the pad (32° in this case) and angular locations in the full core case (45°, 135°, 225°, and 315°). In this Fig. 2, only the pad at 315° is shown. Several moderator regions can be seen outside the vessel. While this is not true to reality, it is likely that replacing these with void regions would cause convergence and stability issues with the 2D/1D method. Since the problems evaluated in this paper are only 2D, the fully integrated 2D/1D method is not used in this work. However, it is ultimately the target solver for this capability, so considerations are made with regard to its potential performance.

It can also be seen in Fig. 2 that the cylindrical representation is pixelated because the entire pin is conditionally being filled with structural material. While this can contribute to some error versus a smoother curvilinear representation, the effect is likely very small. In the results section, some BOL comparisons are made with KENO using a curvilinear representation, and excellent agreement is observed.

In the results section, comparisons between the baffle-only (Fig. 1), full reflector (Fig. 2), and barrel/pad (Fig. 3), are shown. These results help justify that full vessel representation is unnecessary for core physics calculations. However, it is still valuable for vessel fluence calculations.

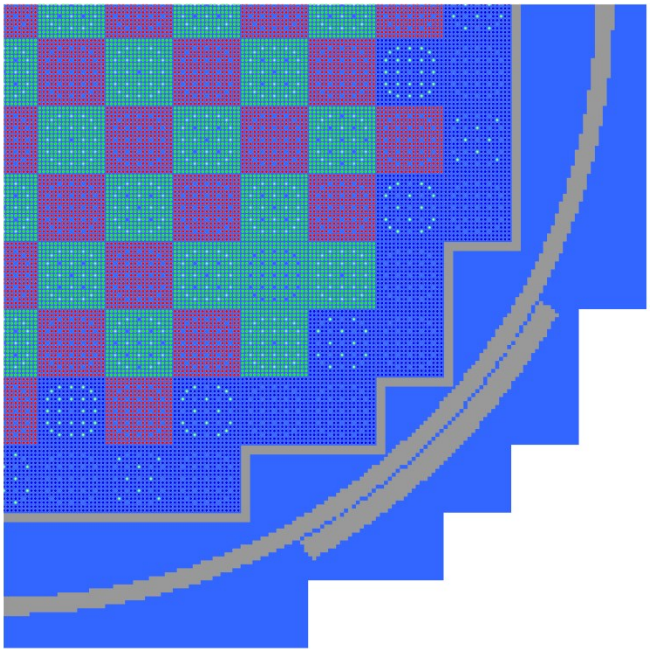

Fig. 3. Geometry visualization of VERA Problem 5a-2D with more core barrel, neutron pad, but without the vessel.

Figures 2 and 3 show that the problem size has increased compared to the baffle-only reflector model in Fig. 1. In Fig. 2, roughly three additional assembly-width of the moderator are necessary, substantially increasing the area of the problem. Figure 3 shows that only a single assembly is added over the baffle-only case. To optimize the computational performance, a partial representation of the core barrel and neutron pad has been introduced, as shown in Fig. 4. This maintains the original problem size shown in Fig. 1 while modeling as much as possible of the structural components. In the Section III, partial representations are indicated by the term *truncated*.

The results show that the truncated representation captures almost all of the effect of having a full representation, so this approach has been adopted as the default behavior in MPACT.

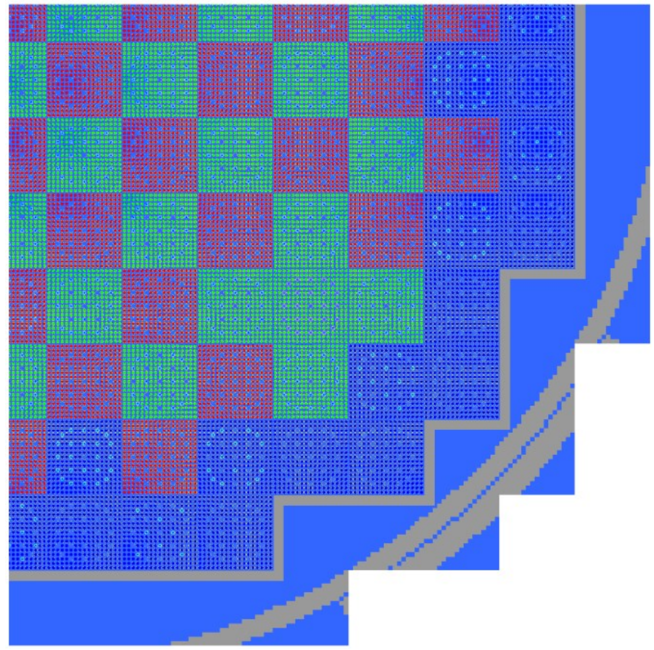

Fig. 4. Geometry visualization of VERA Problem 5a-2D with core barrel, neutron pad, and vessel without additional geometry modules as in the baffle-only case.

III. RESULTS

1. WBN1, 2D Quarter-Core (Problem 5a-2D)

Table I shows the results comparing the four different models presented in the previous section: (1) Baffle-Only, which was the pre-existing model with baffle and assembly-width of reflector, (2) Barrel/Pad (Trunc.), meaning the barrel and pad are modeled, but the problem size is consistent with Baffle-Only, (3) Barrel/Pad (Full), which allows the problem size to expand to fully encompass the barrel and pad, and (4) the full reflector model including the vessel. All results are shown with respect to the full reflector model.

Table I. Results for Problem 5a-2D at BOL Compared to Full Vessel Representation

Reflector Model	Eig.	dk (pcm)	Pin Power RMS (%)	Pin Power MAX (%)	Time (core-hrs)
Baffle-Only	1.00298	-4.1	0.22	1.05	3.19
Barrel/Pad (Truncated)	1.00302	-0.5	0.02	0.07	3.30
Barrel/Pad (Full)	1.00302	-0.2	0.02	0.05	4.11
Full Reflector	1.00302	---	---	---	12.73

As can be seen, the impact of the various reflector models on eigenvalue is fairly negligible, while the impact on power distribution is noticeable. Comparing the baffle-only model to the full reflector shows a 0.2% root mean square (RMS) difference and slightly over 1% maximum pin power errors. The truncated model with the barrel and pad captures the most of the effect, resolving a substantial amount of the inconsistencies. Similar results were also observed in the other two cases in this paper, but a comparable assessment for those is not included here.

A similar study was performed with CE KENO IV [9] comparing the baffle-only and the full reflector model. This study shows consistent findings to those observed here, as in a -4 pcm eigenvalue difference, 0.19% (± 0.08%) RMS pin power error, and 1.01% (±0.17%) MAX error from Godfrey 2014 [9], providing additional validation to the reflector modeling extensions implemented in VERA.

Figure 5 shows the distribution of pin power differences comparing the two cases: baffle-only minus full reflector. Not surprisingly, the baffle-only model under-predicts the pin powers near the periphery along the 45° angle, where the barrel and neutron pad are closest to the fuel.

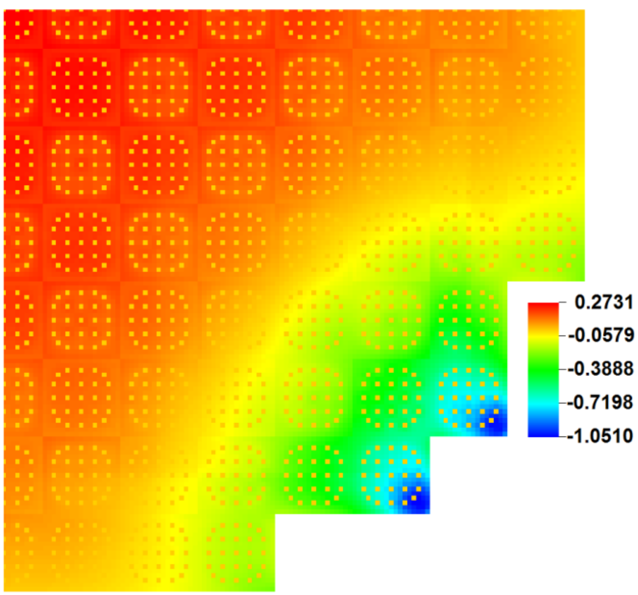

Fig. 5. Pin power comparison (%) at BOC for VERA Problem 5a-2D between baffle-only and full vessel representation.

The power with some core loading patterns can redistribute towards the periphery during the depletion, thereby making the impact of the radial reflector modeling more substantial. To gain further understanding of this effect, the 5a-2D case was depleted for 440 effective full power days (EFPDs) using 20 EFPD timesteps. Since previous results indicate that the truncated barrel/pad model sufficiently captured the effects of the explicit reflector, only the truncated model is used for comparison. Table II provides the results comparing the baffle-only model to the barrel/pad (truncated) model. These results show that the pin power RMS decreases with burnup, while the maximum pin power difference decreases until halfway the cycle and then slowly increases until the end of the cycle.

Table II. Results for Problem 5a-2D with Depletion, Comparing Truncated and Baffle-Only Model

EFPD	GWd/MT	dk (pcm)	RMS (%)	MAX (%)
0	0	-4	0.199	1.003
10	0.38	-4	0.178	1.002
20	0.77	-3	0.175	0.971
40	1.54	-3	0.166	0.931
60	2.30	-3	0.157	0.912
80	3.07	-3	0.148	0.901
100	3.84	-3	0.141	0.895
120	4.61	-3	0.134	0.892
140	5.38	-3	0.128	0.892
160	6.14	-3	0.123	0.893
180	6.91	-4	0.118	0.896
200	7.68	-4	0.114	0.901
220	8.45	-4	0.110	0.908
240	9.22	-4	0.106	0.917
260	9.99	-4	0.103	0.928
280	10.75	-5	0.101	0.941
300	11.52	-5	0.099	0.955
320	12.29	-5	0.098	0.971
340	13.06	-5	0.098	0.989
360	13.83	-5	0.097	1.007
380	14.59	-5	0.097	1.024
400	15.36	-5	0.097	1.004
420	16.13	-6	0.097	1.057
440	16.90	-6	0.097	1.073

2. Krško, 2D Quarter-Core

Simulations of the Krško core are of interest for VERA validation because the smaller core (2-loop core with 121 assemblies) and the dryer lattice compared to typical PWR fuel challenge power distribution and reactivity predictions [10]. This increases the importance of the radial reflector compared to larger cores (e.g., WBN1). The 16 × 16 assemblies featured by this core have an asymmetric guide tube configuration which imposes full-core simulations to retain the actual core configuration. Despite this, geometry figures for this core are shown in quarter symmetry to be consistent with previous figures and to emphasize the reflector region.

As in Figure 2, Figure 6 shows the geometry visualization of a 2D slice of the Krško Cycle 1 core, including all reflector components out to the vessel. In the WBN1 core, the core barrel and pad came closest to the assemblies along the diagonal of the core. In this design, however, these components come closest to the assemblies along the *x*- and *y*-axes, so a higher power distribution impact at these locations should be expected.

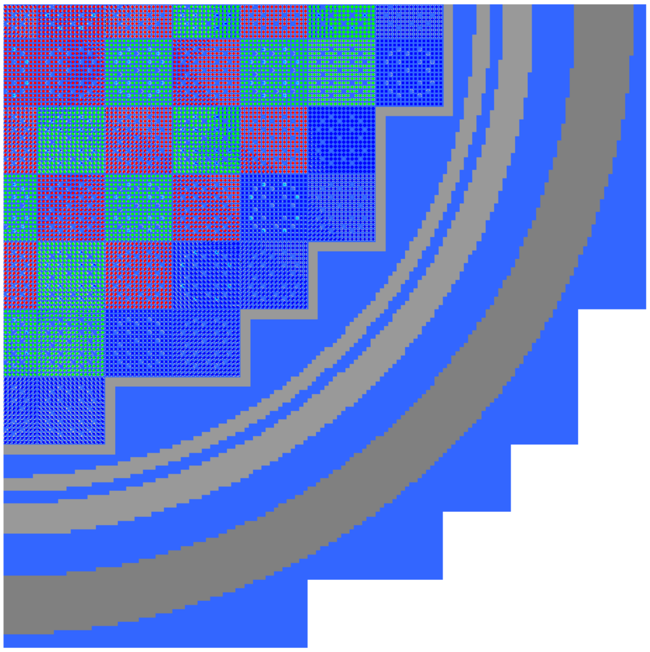

Fig. 6. Geometry visualization of the 2D Krško core with core barrel, neutron pad, and vessel.

Figure 7 shows a similar representation, but the problem size is truncated to avoid adding computational burden over the baffle-only case. WBN1 results show that this truncated model performed very well compared to the full model, so it will be used for the comparisons herein.

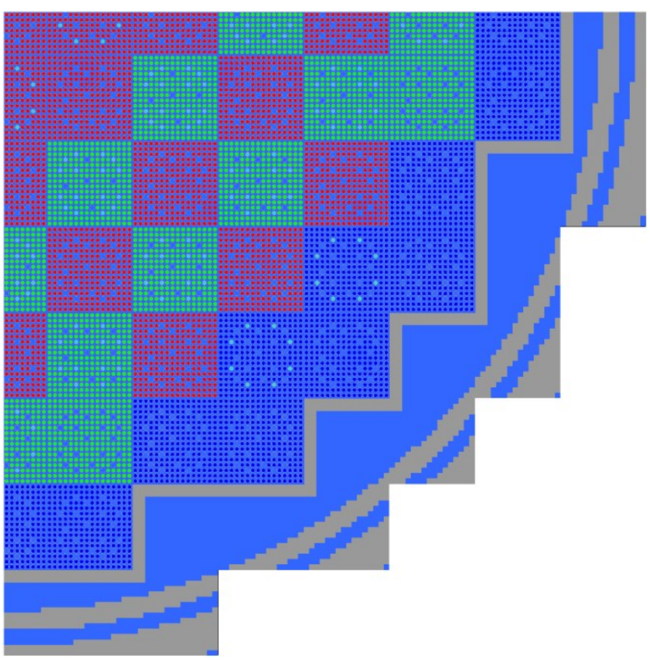

Fig. 7. Geometry visualization of the 2D Krško core with core barrel, neutron pad, and vessel without additional geometry modules.

Table III shows the results comparing the truncated model depicted in Fig. 7 to the baffle-only model for a cycle depletion of 440 EFPD in in 20 EFPD steps. From these results, a more significant effect on reactivity and power distribution is observed compared to WBN1. While higher pin power differences are observed near BOC, a slightly larger reactivity bias is observed near EOC. The reactivity bias is still low (<20 pcm), but it is roughly three times higher than the value for the WBN1 analysis. The RMS of the pin power difference is roughly twice as high, though the maximum difference is roughly the same at slightly above 1%.

Table III. Results for 2D Krško core with depletion.

EFPD	GWd/MT	dk (pcm)	RMS (%)	MAX (%)
0	0	-14	0.427	1.394
10	0.38	-14	0.391	1.339
20	0.77	-13	0.383	1.304
40	1.54	-12	0.362	1.249
60	2.30	-12	0.341	1.210
80	3.07	-12	0.323	1.180
100	3.84	-12	0.307	1.155
120	4.61	-12	0.293	1.135
140	5.38	-12	0.281	1.118
160	6.14	-13	0.271	1.103
180	6.91	-13	0.262	1.096
200	7.68	-13	0.254	1.092
220	8.45	-14	0.247	1.090
240	9.22	-14	0.241	1.090
260	9.99	-15	0.236	1.092
280	10.75	-15	0.232	1.097
300	11.52	-16	0.229	1.104
320	12.29	-16	0.227	1.112
340	13.06	-17	0.225	1.121
360	13.83	-17	0.224	1.132
380	14.59	-18	0.224	1.143
400	15.36	-18	0.224	1.155
420	16.13	-18	0.224	1.167
440	16.90	-19	0.224	1.179

Figures 8 and 9 show the full symmetry pin power difference distributions at BOC and EOC, respectively, based on the pin power from the baffle-only case minus those from the truncated reflector case. Since the reflector structural components come closest to the fuel along the *x*- and *y*-axes, the maximum pin power discrepancies are observed there, and there is a more subtle but appreciable effect on the power distribution in the center of the core. As the cycle depletes, however, the magnitude of this impact shrinks, and the largest differences are localized to the pins closest to the core periphery.

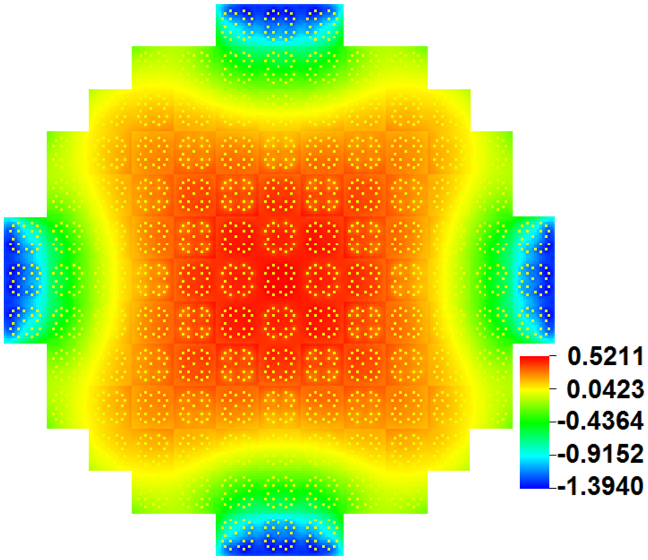

Fig. 8. Pin power comparison (%) at BOC for the 2D Krško core between baffle-only and truncated representation.

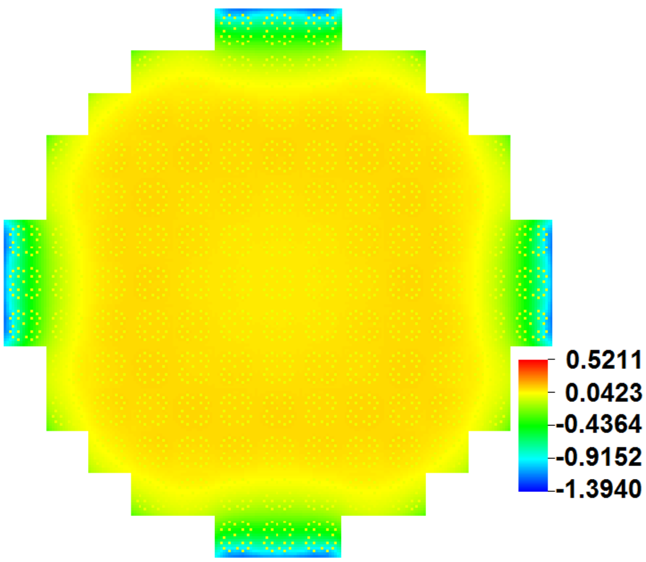

Fig. 9. Pin power comparison (%) at EOC for the 2D Krško core between baffle-only and truncated representation.

3. AP1000, 2D Quarter-Core with Shroud Ring

As a key partner of CASL, Westinghouse has used VERA to simulate the AP1000 core design [11,12]. The AP1000 core's advanced core configuration [13] has been instrumental in helping advance the accuracy and capabilities of VERA [14]. Figure 10 shows the core layout [13], which contains a large variation in the average enrichment of each assembly ranging from 0.74% ^{235}U to 4.38% ^{235}U.

As in the Krško core, the reflector components come closest to the assemblies along the *x*- and *y*-axes. One noteworthy feature for this study is the axially varying shroud rings, which are even closer than the barrel in WBN1. The localized effect on the power of the pins closest to the shroud ring is expected to be significant.

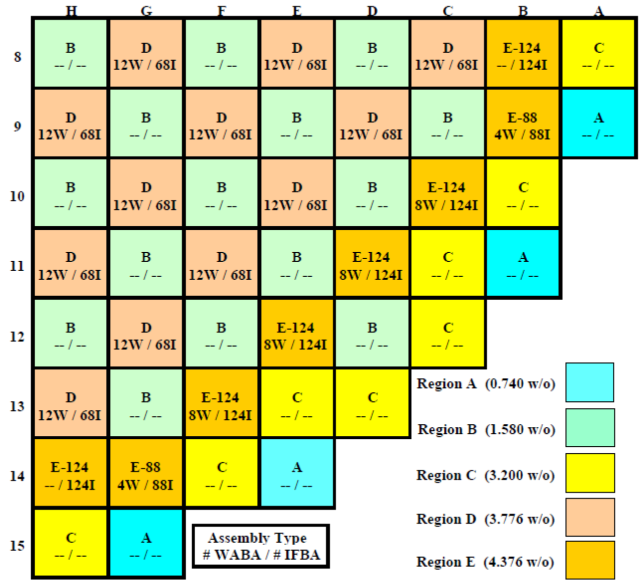

Fig. 10. Assembly layout of the AP1000 core [13].

For comparison to the MPACT model, Figure 11 shows the KENO model for the core with all reflector components out to the vessel. A 1-inch thick shroud ring can be seen just inside the core barrel and the core pads, which are located every 90° and have tapered edges.

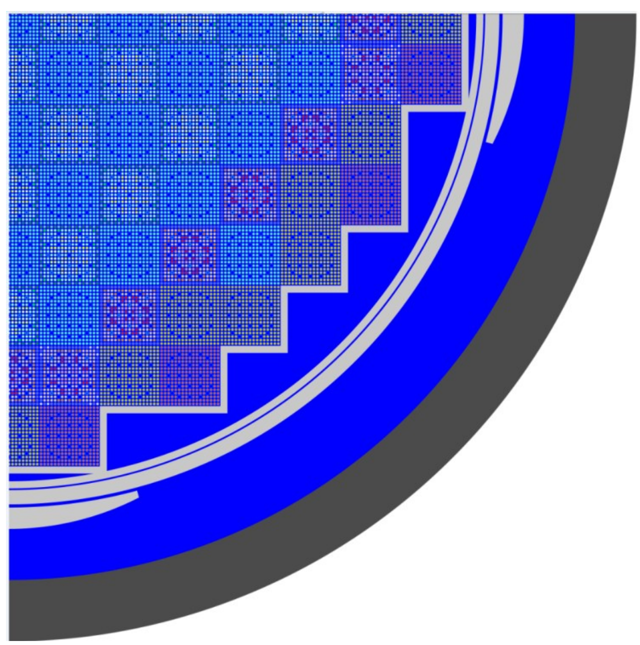

Fig. 11. KENO model showing the reflector components in the 2D AP1000 quarter-core model with shroud ring.

Figure 12 shows the corresponding MPACT model. The tapered edges of the core pads are not currently supported in the capability, but it could be considered in future improvements. However, as will be seen in the results, it is unlikely that the tapered edges will have any significant effect on the results.

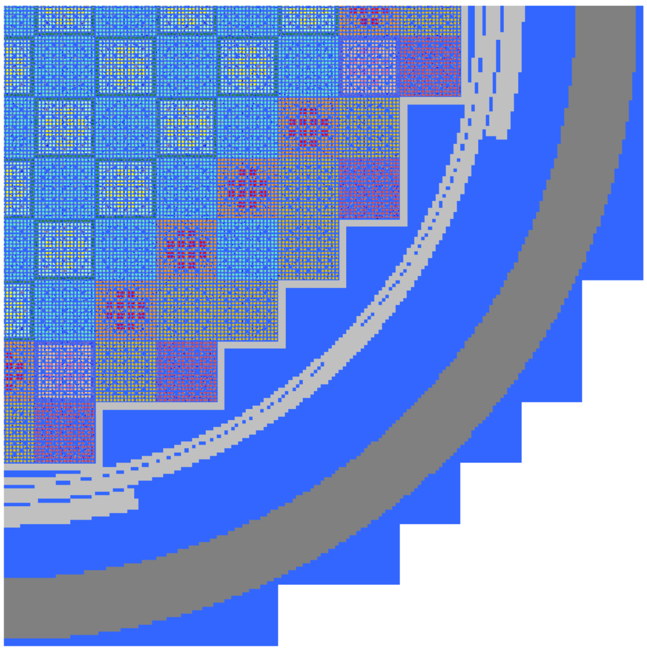

Fig. 12. MPACT model showing the reflector components in the 2D AP1000 quarter-core model with shroud ring.

Table IV shows the results for this case. A 0.5 GWd/MT burnup step size was used for the cycle depletion, but for conciseness, the results are shown every 1.0 GWd/MT. As in both the WBN1 and Krško cases, the reactivity bias from the reflector modeling type increases as the cycle is depleted, but is notably larger in the AP1000 simulation (~2 times larger than in Krško and 6 times larger than WBN1, respectively). A substantially larger impact on the pin power distribution is observed for the AP1000 simulation, particularly at BOC, where the impact of the reflector modeling choice on the maximum pin power difference is almost 3.5% (roughly 3 times larger than in previous cases).

Table IV. Results for the 2D AP1000 case with depletion.

GWd/MT	dk (pcm)	RMS (%)	MAX (%)
0.00	-12	0.644	3.488
1.00	-14	0.618	3.628
2.00	-17	0.582	3.757
3.00	-18	0.516	3.771
4.00	-19	0.440	3.649
5.00	-19	0.385	3.449
6.00	-20	0.354	3.224
7.00	-21	0.328	3.061
8.00	-22	0.310	2.993
9.00	-24	0.303	2.994
10.00	-26	0.301	3.034
11.00	-28	0.302	3.095
12.00	-30	0.305	3.161
13.00	-31	0.308	3.224
14.00	-33	0.310	3.268
15.00	-34	0.311	3.319
16.00	-36	0.311	3.340
17.00	-36	0.310	3.372
18.00	-37	0.308	3.428
18.66	-37	0.306	3.456

Figures 13 and 14 show the pin power difference distributions at BOC and EOC, respectively. As expected, the pin power difference is largest at the periphery along the *x*- and *y*-axes. The power differences in the natural U assemblies at A-9 and G-15 are substantially lower than in the neighboring assemblies because of the low power in the natural U assemblies.

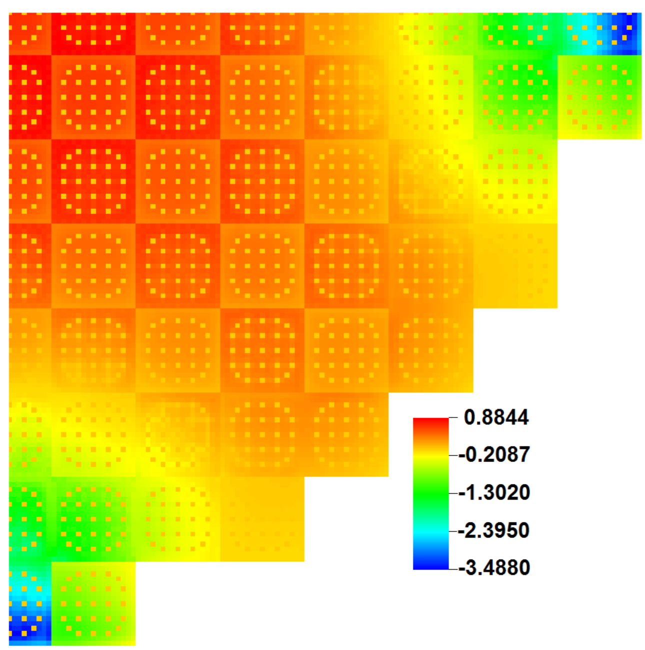

Fig. 13. Pin power comparison (%) at BOC for the 2D AP1000 core between baffle-only and truncated representation.

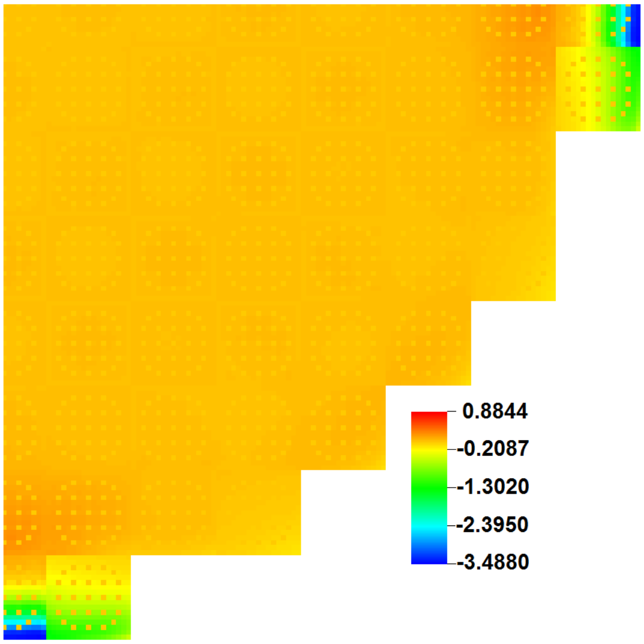

Fig. 14. Pin power comparison (%) at EOC for the 2D AP1000 core between baffle-only and truncated representation.

Comparing to the 2D CE-KENO VI model with full reflector from Fig. 11 at BOC, the MPACT results show notable improvement, particularly with respect to the maximum pin power difference. Comparing the baffle-only model, the eigenvalue difference is -187 pcm with a 0.662% pin power RMS and 2.905% MAX. With the improved reflector capability, the new results are at -176 pcm, 0.534% RMS and 1.218% MAX.

IV. CONCLUSIONS AND FUTURE WORK

This paper presents recent improvements to the radial reflector modeling capabilities in MPACT, the deterministic solver of VERA. Improvements were made through development of the simple pin-based structural cylinder model. The impacts of several reflector modeling choices are described and applied to the WBN1 core model, including a full reflector model encompassing a core barrel, neutron pad, and vessel. This allowed a computationally effective geometrical approximation of the reflector to be adopted. By properly truncating the reflector region outside the baffle, the sizes of the current models are preserved, incorporating an adequate amount of reflector structures to obtain the desired accuracy. The truncated approach has been demonstrated to yield notable improvements in the power distribution prediction for the peripheral pins over VERA's prior modeling choice for the reflector, which consisted of only the baffle and an assembly-width of moderator. In general, the effect of the reflector model on eigenvalue proved small, even throughout the depletion.

2D core configurations based on the Krško and AP1000 designs with various reflector models were also tested. Krško is a 121-assembly 2-loop core, which is smaller than the WBN1 193-assembly 4-loop core. Therefore, the importance of the radial reflector is more significant. This determination is supported by the results of the analysis. The AP1000 core has an axially varying shroud ring located in the proximity of the core periphery. While the 2D core model analyzed in this work does not account for the axial dependence of the shroud, its modeling impact proved significant.

Compared to WBN1, a larger reactivity impact due to the refined reflector model is observed to be up to ~20 pcm for Krsko and up to 40 pcm for the AP1000 compared to <10 pcm in WBN1. Since the analysis has been performed only for cycle 1 and the reactivity impact typically increases during the depletion, subsequent reloads may show a larger reactivity impact due to the depletion histories of the shuffled assemblies.

Future work will focus on extending the testing to 3D cases. Preliminary analysis for a WBN1 3D core model shows pin power differences in excess of 3% vs 1% in the corresponding 2D model. Incorporating the ability to model an axially heterogeneous shroud will allow for a more accurate representation of the AP1000 core. This capability will also be relevant to planned analysis of vessel fluence to be performed with VERA.

ACKNOWLEDGMENTS

This research was supported by the Consortium for Advanced Simulation of Light Water Reactors (www.casl.gov), an Energy Innovation Hub (http://www.energy.gov/hubs) for Modeling and Simulation of Nuclear Reactors under US Department of Energy Contract No. DE-AC05-00OR22725.

The authors express their gratitude to the NPP Krško and JSI personnel for their support during the project.

All figures except for Figs. 10 and 11 were generated using the VisIt software package [15].

REFERENCES

1. "Consortium for Advanced Simulation of Light Water Reactors (CASL)." Available online. URL http://www.casl.gov/ (2015).
2. J. TURNER et al., "The Virtual Environment for Reactor Applications (VERA): Design and architecture," *Journal of Computational Physics*, **326**, 544 (2016).
3. B. COLLINS et al., "Stability and Accuracy of 3D Neutron Transport Simulations Using the 2D/1D Method in MPACT," *Journal of Computational Physics*, **326**, 612 (2016).
4. MPACT Team, "MPACT Theory Manual, Version 2.0.0," Tech. Rep. CASL-U-2015-0078-000, Oak Ridge National Laboratory and University of Michigan (2015).

5. H. G. JOO et al., “Methods and Performance of a Three-Dimensional Whole-Core Transport Code DeCART,” *Proc. PHYSOR 2004*, American Nuclear Society, Chicago, IL (2004).
6. Y. S. JUNG et al., “Practical numerical reactor employing direction whole core neutron transport and subchannel thermal/hydraulic solvers,” *Annals of Nuclear Energy*, **62**, 357 (2013).
7. S. STIMPSON, B. COLLINS, and T. DOWNAR. “Axial Transport Solvers for the 2D/1D Scheme in MPACT,” *Proc. PHYSOR 2014*, Kyoto, Japan (2014).
8. K. S. KIM et al., “Development of a New 47-Group Library for the CASL Neutronics Simulators,” *Proc. M&C 2015*, Nashville, Tennessee (2015).
9. A. T. GODFREY, “VERA Core Physics Benchmark Progression Problem Specifications (Rev. 4),” Tech. Rep. CASL-U-2012-0131-004, Oak Ridge National Laboratory (2014).
10. A. GODFREY et al., “VERA Benchmarking Results for KRŠKO Nuclear Power Plant Cycle 1,” *Proc. PHYSOR 2016*, Sun Valley, Idaho, USA (May 1–5, 2016).
11. F. FRANCESCHINI et al., “AP1000 PWR Reactor Physics Analysis with VERA-CS and KENO-VI – Part II: Power Distribution,” *Proc. PHYSOR 2014*, Kyoto, Japan, September 28–October 3 (2014).
12. D. SALAZAR et al., “AP1000® PWR Cycle 1 HFP Depletion Simulations With VERA-CS,” *Proc. PHYSOR 2016*, Sun Valley, Idaho, USA (May 1–5, 2015).
13. M. HONE et al., AP1000 Core Reference Report, Westinghouse Electric Company, WCAP-17524-NP (March 2012).
14. S. STIMPSON et al., “Improved Diffusion Coefficients for SP_N Axial Solvers in the MPACT 2D/1D Method Applied to the AP1000® PWR Start-Up Core Models,” *Proc. M&C 2015*, Nashville, Tennessee, USA (April 19–23, 2015).
15. H. CHILDS et al., “VisIt: An End-User Tool for Visualizing and Analyzing Very Large Data,” High Performance Visualization – Enabling Extreme-Scale Scientific Insight, pp. 357–372 (2012).